Conduction band states of transition metal (TM) high-*k* gate dielectrics as determined from X-ray absorption spectra

G. Lucovsky [a,b,*], J.G. Hong [b], C.C. Fulton [b], N.A. Stoute [a], Y. Zou [a],
R.J. Nemanich [a], D.E. Aspnes [a], H. Ade [a], D.G. Schlom [c]

[a] *Department of Physics, North Carolina State University, Raleigh, NC 27695, USA*
[b] *Department of Materials Science and Engineering, North Carolina State University, Raleigh, NC 27695, USA*
[c] *Department of Materials Science, Pennsylvania State University, State College, PA, USA*

Abstract

This paper uses X-ray absorption spectroscopy to study the electronic structure of the high-*k* gate dielectrics including TM and RE oxides. The results are applicable to TM and rare earth (RE) silicate and aluminate alloys, as well as complex oxides comprised of mixed TM/TM and TM/RE oxides. These studies identify the nature of the lowest conduction band d* states, which define the optical band gap, E_g, and the conduction band offset energy with respect to crystalline Si, E_B. E_g and E_B scale with the atomic properties of the TM and RE atoms providing important insights for identification high-*k* dielectrics that meet performance targets for advanced CMOS devices.
© 2004 Published by Elsevier Ltd.

1. Introduction

The paper presents a study electronic structure in high-*k* TM oxides by X-ray absorption spectroscopy and vacuum ultra-violet spectroscopic ellipsometry. Combined with X-ray photoelectron spectroscopy and Auger electron spectroscopy, these results are applied to band alignments at Si-high-*k* dielectric interfaces, not only for the Ti, Zr and Hf oxides, but to other TM/RE oxides, silicates and aluminates [1,2].

2. Experimental spectra

Fig. 1(a) is the Zr $M_{2,3}$ spectrum. Ti $L_{2,3}$ and Hf $M_{2,3}$ spectra are similar, and quantitative differences will be

addressed. Features in the Zr $M_{2,3}$ spectrum are replicated for spin–orbit split initial p states, $3p_{1/2}$ and $3p_{3/2}$. For each of these p states, there are transitions to a 4d* state doublet and a 5s* state singlet at higher energy. The Ti $L_{2,3}$ 3d* and Zr $M_{2,3}$ 4d* doublet features are resolved, but the 5d* doublet of the Hf $N_{2,3}$ spectra is not. The d* doublet splittings, $\Delta(d^*_{1,2})$, for Ti and Zr, are essentially the same, 2.1 ± 0.2 eV, and the splittings between the lower d* state, d^*_1, and the s* state, $\Delta(d^*_1, s*)$, differ by <1 eV; 12.6 ± 0.2 eV for TiO$_2$, and 11.8 ± 0.2 eV for ZrO$_2$. Finally, the experimental spin–orbit splittings are 5.6 eV ± 0.3 eV for the Ti 2p states, 13.3 ± 0.3 eV for the Zr 3p states and for 57.6 eV ± 0.3 eV for the Hf 4p states.

The relative absorption strengths for the d* and s* features in the p state spectra for TiO$_2$, ZrO$_2$ and HfO$_2$ are markedly different. The s* state spectral features are relatively weak in the TiO$_2$ L_3 and L_2 spectra, increase modestly for the ZrO$_2$ M_3 and M_2 spectra, and are stronger for the HfO$_2$ $N_{2,3}$ spectra.
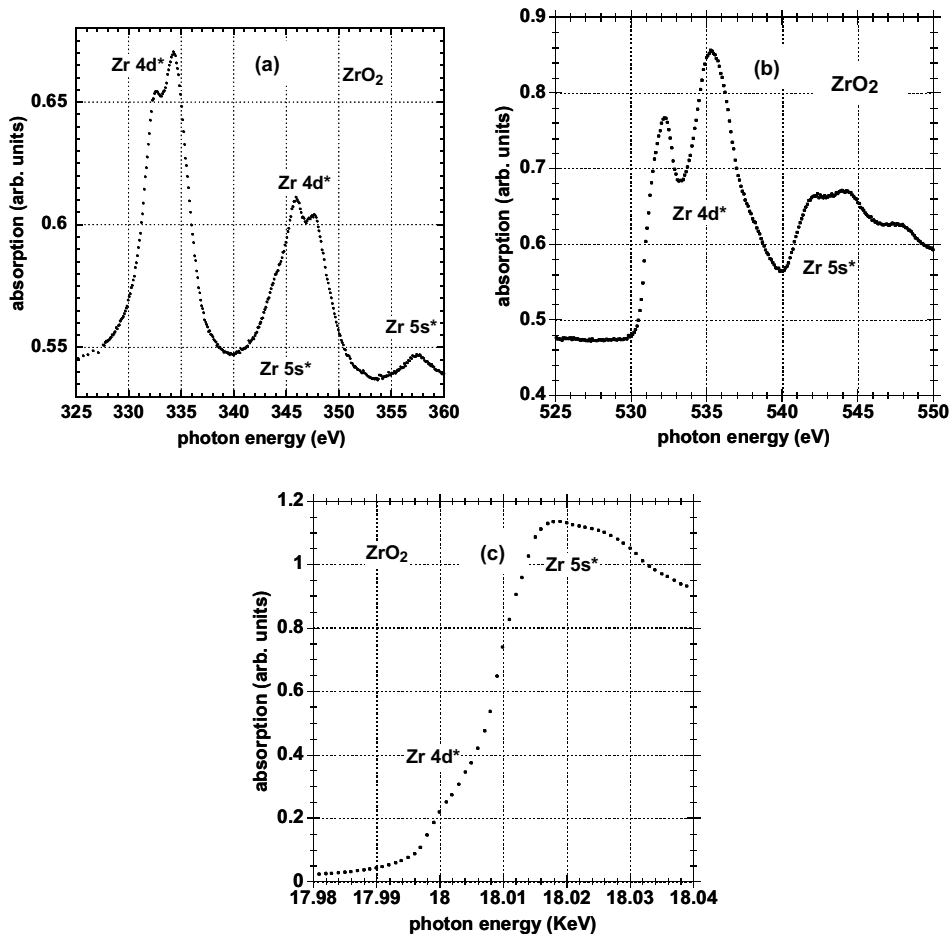
Fig. 1. ZrO$_2$ spectra: (a) Zr M$_{2,3}$, (b) O K$_1$, (c) Zr K$_1$.

Fig. 1(b) is the O K$_1$ spectra for ZrO$_2$. The O K$_1$ spectra for TiO$_2$, ZrO$_2$ and HfO$_2$ are similar, displaying a well-resolved d* doublet at the absorption threshold, and a broader s* feature with some additional structure at higher energies. The $\Delta(d^*_{1,2})$ splitting increases from 2.7 eV in TiO$_2$ to 3.2 eV in ZrO$_2$ then to 4.3 in HfO$_2$. The spectral overlap between the higher energy d* state, d$_2$, and the lowest energy s* feature decreases from TiO$_2$ and ZrO$_2$, to HfO$_2$.

The Zr K$_1$ spectrum for ZrO$_2$ is shown in Fig. 1(c) and is similar spectra presented in Ref. [3]. Since transitions from the Zr 1s-state to Zr 4d* and 5s* states are not dipole-allowed, the Zr K$_1$ edge spectrum is qualitatively similar to the O K$_1$ edge spectrum in which the final states are a mixture of (i) Zr 4d* and 5s* states, and (ii) O 2p* states. The doublet 4d* features are not resolved in Fig. 3, or in Ref. [3]. The average d*–s* energy difference is ~10 eV.

Ti K$_1$ and Hf K$_1$ edge spectra have not been obtained for the thin film samples prepared for this study. How-

ever, there have been published studies of the Ti K$_1$ edge in the rutile and anatase crystal forms of TiO$_2$ [4]. A comparison indicates a similar energy dependence between the O K$_1$ spectra for the nano-crystalline TiO$_2$ film of this study, and the published rutile Ti K$_1$ spectrum. The d state splittings are the same to within experimental error: 2.5 ± 0.3 eV for the Ti K$_1$ spectrum, and 2.7 ± 0.3 eV for the O K$_1$ spectrum as are average differences in energy between the d$^*_1$ state feature and the first s* state spectral peak: 8.6 ± 0.3 eV for the Ti K$_1$ spectrum, and 8.4 ± 0.3 eV for the O K$_1$ spectrum. However, as in the case of ZrO$_2$, the relative intensities of the d* and s* features are different in the Ti K$_1$ and O K$_1$ spectra.

Fig. 2 contains a plot of the optical absorption constant, α, versus photon energy for ZrO$_2$, as obtained from an analysis of vacuum ultra-violet spectroscopic ellipsometry data. The threshold for optical absorption is at ~5.7 eV, essentially the same as reported from measurements of the photoconductivity [5]. Relatively broad
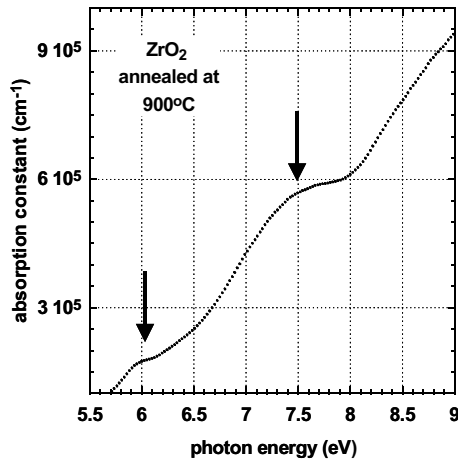
Fig. 2. Band edge spectrum for ZrO_2.

features assigned to d^* state absorptions are centered at ∼6.0 eV and ∼7.5 eV. The spectral peak associated with transitions to the $5s^*$ band occurs beyond the spectral range of these studies. The d^* spectral features in the absorption edges of HfO_2 and TiO_2 are similar to those of ZrO_2 [4,6].

3. Analysis of experimental results

Using spectra for ZrO_2 as an example, this section distinguishes between the intra-atomic Zr $M_{2,3}$ spectrum of Fig. 1(a) and the (i) O K_1 spectrum of Fig. 1(b), (ii) the Zr K_1 spectrum of Fig. 1(c), and (iii) the band edge absorption spectrum of Fig. 2. These distinctions are supported by ab initio calculations performed on relative small clusters centered on either (i) the Zr-atoms for the Zr $M_{2,3}$, and K_1 spectra, or (ii) the O-atoms for the O K_1 and band edge spectra [7]. Similar distinctions apply to TiO_2 and HfO_2.

The Ti $L_{2,3}$, Zr $M_{2,3}$ and Hf $N_{2,3}$ edge spectra are due to intra-atomic transitions from relatively deep spin–orbit split Ti 2p-, Zr 3p- and Hf 4p-states to empty 3, 4 or $5d^*$- and 4, 5 or $6s^*$-states, respectively. These intra-atomic transitions are not significantly changed by 2nd neighbors as shown for the Zr $M_{2,3}$ spectra through the comparisons with homogeneous, as well as phase-separated Zr silicate alloys [1]. The relative intensities of final d^*-states in the Ti and Zr spectra are consistent final state effects due to core hole localization. The relative strengths of the d^* and s^* absorptions in the spectra for TiO_2, ZrO_2 and HfO_2 are markedly different, butr are in qualitative agreement with relative intensities based on Rydberg states. [8].

The O K_1 edge spectra for TiO_2, ZrO_2 and HfO_2 are due inter-atomic transitions from O 1s-core states to final *band-like* states with a mixed (i) O $2p^*$-state, and (ii) TM 3, 4 or 5 d^*- and TM 4, 5 or 6-s^*-state character. In contrast to order of magnitude intensity variations between the respective, (i) Ti and Zr, and (ii) Hf d^* and s^* spectral features in Fig. 1, the d^* and s^* related features in Fig. 1(b) display intensities that differ by less than a factor of two demonstrating that matrix elements for absorption to d^* and s^* state features in O K_1 spectra are not determined by Rydberg-like transition probabilities, but instead by the mixed character of the final states.

The Zr K_1 (Fig. 1(c)), and the Ti and Zr K_1 spectra discussed in Refs. 4,5 and 6 are also inter-atomic spectra. The transitions between the Zr and Ti 1s-states to the respective Zr $4d^*$ and $5s^*$ states, and Ti $3d^*$ and $4s^*$ states are not dipole-allowed, and the lowest energy transitions are to final states with a mixed O $2p^*$ state, and Ti or Zr d^* and s^* state character. This interpretation is supported by noting that these transitions have features at higher energy that are used in extended X-ray absorption fine structure (EXAFS) studies to determine nearest neighbor Zr and O, and Ti and O bond lengths, and second and more distant neighbor inter-atomic separations as well [9].

Even though the final states have similar atomic character, the relative absorptions of the $4d^*$ and $5s^*$ features in the O K_1 and Zr K_1 spectra of ZrO_2 are markedly different. These differences reflect differences in the respective O 1s- and Zr 1s ground state wave functions, and their effect on the transition probabilities for these absorptions. This comparison also holds for the relative absorptions of the $3d^*$ and $4s^*$ features in the O K_1 and Ti K_1 spectra of TiO_2.

Finally, comparisons between the energies of the first spectral peak of the respective O K_1 spectra, 530.1 eV for TiO_2, 532.4 eV for ZrO_2, and 532.6 for HfO_2, indicate that the differences between energies are equal to within an uncertainty of ±0.3 eV to the respective differences in reported *nominal band gap energies* of 3.1 eV for rutile TiO_2 [10], 5.6 eV for ZrO_2 [5], and 5.8 eV for HfO_2 [5]. This comparison carries over as well to high-k complex oxide such as $GdScO_3$ [11].

4. Discussion of band offset energies and tunneling

There has been a search for alternative dielectrics with significantly increased dielectric constants, k, with respect to SiO_2 to reduce direct tunneling in FETs with EOT < 1.5 nm. This allows increases in physical thickness proportional to k for a given gate dielectric capacitance, thereby providing the possibility of significantly reduce direct tunneling. However, *increases* in k are accompanied by *decreases* in E_g, E_B, and the electron tunneling mass, m_{eff}^*. These trade-offs are

quantified in a tunnelling figure of merit [12], Φ_m, given by Eq. (1),

$$\Phi_m = k[E_B \cdot m^*_{eff}]^{0.5}. \tag{1}$$

Robertson has developed a model for obtaining band gaps and band offset energies for dielectrics including the high-k dielectrics of this paper [13]. These results yield an approximately linearly relation for E_B as a function of E_g. Fig. 3(a) contains plots of E_g and E_B as a function of the atomic d state energy for a representative set of TM oxides. The scaling in Fig. 3(a) follows directly from the spectroscopic studies of this paper, and ab initio calculations that are being performed. O K_1 spectra of TM oxides provide quantitative information about relative band gaps for TM oxides, and for the extension of this relationship to more complex oxide alloys and compounds as well. Using these comparisons, the TM oxides with the highest dielectric constants,
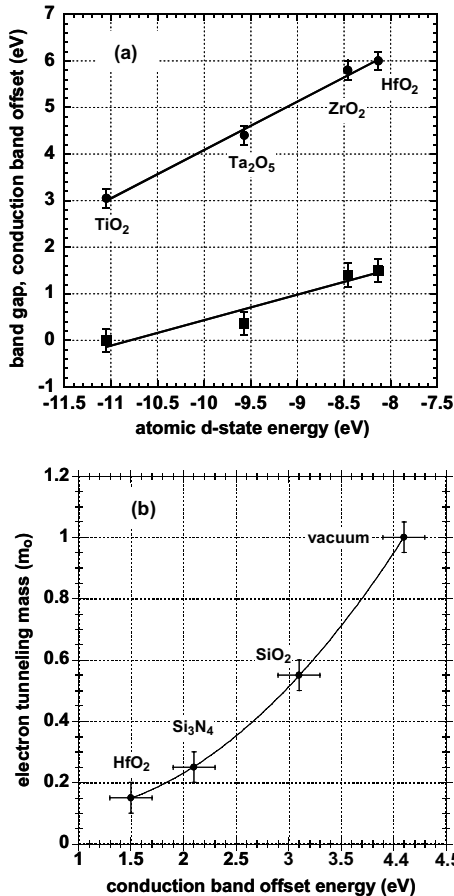
TiO_2, and Nb_2O_3 and Ta_2O_3, have offset energies below 1 eV that either correlate with high tunneling leakage, and/or electric field assisted injection into low-lying conduction band states associated with these atoms [14]. Based on scaling with atomic d-states, (i) the oxides of Zr and Hf and their respective silicate and aluminate alloys, as well as (ii) Y, La and the lanthanide RE oxides, and their silicate and aluminate alloys should have conduction band offset energies >1.2–1.3 eV, and therefore the potential for meeting roadmap targets for low tunneling leakage current [15], provided that the electron tunneling mass, m_{eff}, does not decrease significantly with decreasing E_B.

Fig. 3(b) is a plot of the electron tunneling mass, m_{eff}, versus E_B. The linear portion for E_B between ~2.5 and 4.1 eV is in accord with the Franz two-band model [16], and applies when the conduction band states are free electron-like with predominantly s*-character. The projected values for m_{eff} when E_B is <2 eV are attributed to a change in the character of the lowest conduction band states d* states in the high-k dielectrics; an E_B of 1.2–1.3 eV represents a realistic device scaling limitation.

Acknowledgments

References

[1] Lucovsky G, Hong JG, Fulton CC, Zou Y, Nemanich RJ, Ade H. J Vac Sci Technol B 2004;22:2132.
[2] Rayner GB, Kang D, Lucovsky G. J Vac Sci Technol B 2002;20:1748.
[3] Lim P et al. Phys Rev B 1993;48:10063.
[4] Grunes LA et al. Rev B 1983;25:7157.
[5] Afanas'ev VV et al. In: Houssa M, editor. High-k gate dielectrics. Institute of Physics, Bristol, 2004.
[6] Grunes LA. Phys Rev B 1983;27:2111.
[7] Lucovsky G et al. Appl Phys Lett 2001;79:1775.
[8] Condon EU, Shortly GH. The theory of atomic spectra. Cambridge, UK: Cambridge University Press; 1957 [Chapter V].
[9] Koningsberger DC, Prins RP, editors. X-ray absorption: principles, applications, techniques of EXAFS, SEXAFS and XANES. New York: Wiley; 1988.
[10] Cox PA. Transition metal oxides. Oxford: Oxford Science Publications; 1992 [Chapter 2].
[11] Lucovsky G, Zhang Y, Whitten JL, Schlom DE, Freeouf JL. Physica E 2004;21:712.
[12] Hinkle CL, Fulton CC, Nemanich RJ, Lucovsky G. Microelectron Eng 2004;72:257.
[13] Robertson J. J Vac Sci Technol B 2000;18:1785.
[14] Johnson RS et al. Vac Sci Technol B 2002;20:1126.
[15] ITRS, 2001 ed. Available from: http://public.itrs.net.

Fig. 3. (a) E_g, E_B vs. d-state energy and (b) m_{eff} vs. E_B.